CHEMISTRY
A EUROPEAN JOURNAL

ChemPubSoc
Europe

DOI: 10.1002/chem.201204016

Induction of Motion in a Synthetic Molecular Machine: Effect of Tuning the Driving Force

Jacob Baggerman,[a] Natalia Haraszkiewicz,[a] Piet G. Wiering,[a] Giulia Fioravanti,[b] Massimo Marcaccio,[c] Francesco Paolucci,*[c] Euan R. Kay,[d] David A. Leigh,*[d] and Albert M. Brouwer*[a]

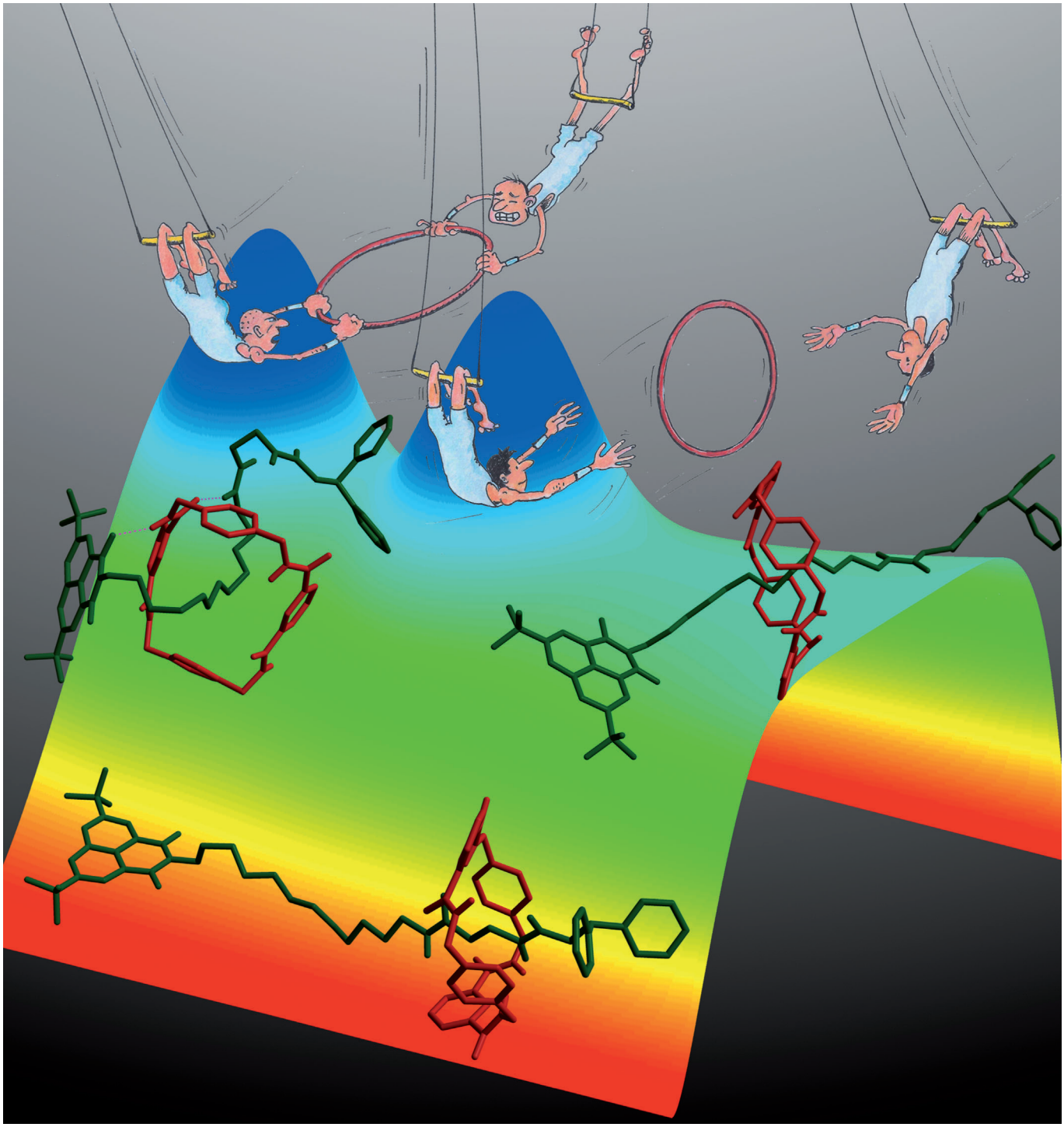

Abstract: Rotaxane molecular shuttles were studied in which a tetralactam macrocyclic ring moves between a succinamide station and a second station in which the structure is varied. Station 2 in all cases is an aromatic imide, which is a poor hydrogen-bond acceptor in the neutral form, but a strong one when reduced with one or two electrons. When the charge density on the hydrogen-bond-accepting carbonyl groups in station 2 is reduced by changing a naphthalimide into a naphthalene diimide radical anion, the shuttling rate changes only slightly. When station 2 is a pyromellitimide radical anion, however, the shuttling rate is significantly reduced. This implies that the shuttling rate is not only determined by the initial unbinding of the ring from the first station, as previously supposed. An alternative reaction mechanism is proposed in which the ring binds to both stations in the transition state.

Keywords: electrochemistry · molecular shuttles · photochemistry · reaction mechanisms · rotaxanes

Introduction

One of the fascinating aspects of motor proteins is their capability to generate directional motion and force,[1–7] and to create molecular systems that behave like such biomolecular motors is a challenge that has been taken up by an increasing number of researchers.[8–27] Rotaxane-based molecular shuttles are a prototypical class of synthetic molecular machines.[19,28–44] They consist of (at least) two components mechanically linked together: a macrocyclic ring, which surrounds a linear unit (thread) with bulky groups (stoppers) at the ends that prevent the macrocycle from slipping off. The two parts can move relatively easily with respect to each other because there is no covalent bonding between them. If the rotaxane has two binding sites ("stations"), then it is possible to move the macrocycle from one station to the other by changing the relative binding affinity of one of the stations. A few years ago, we introduced rotaxane **1**, which showed reversible translational movement on a microsecond timescale. Rotaxane **1** consists of a tetralactam macrocycle around a thread with a succinamide station and a naphthalimide station connected by an alkyl chain. The co-conformation in which the macrocycle is bound to the succinamide group (*succ*-**1**) is by far the most stable one according to

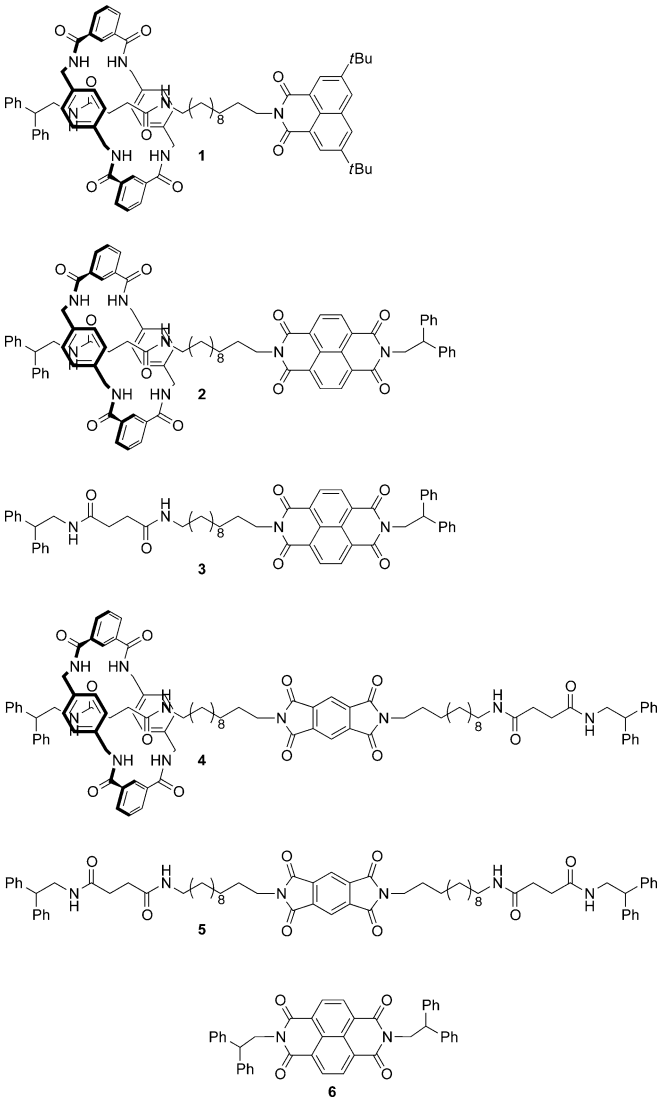

^{1}H NMR[45] and IR spectroscopic studies.[46–48] Reduction of the naphthalimide group leads to a change in the equilibrium position of the macrocycle. It has a higher affinity toward the naphthalimide radical anion (*ni*-**1**$^{\bullet-}$) than for the succinamide station, and moves over on a microsecond timescale.[49]

[a] Dr. J. Baggerman, Dr. N. Haraszkiewicz, P. G. Wiering, Prof. Dr. A. M. Brouwer
Van 't Hoff Institute for Molecular Science
University of Amsterdam, P.O. Box 94157
1090 GD Amsterdam (The Netherlands)
E-mail: A.M.Brouwer@uva.nl

[b] Dr. G. Fioravanti
Department of Physical and Chemical Sciences
University of L'Aquila, Via Vetoio 1, 67100 L'Aquila (Italy)

[c] Dr. M. Marcaccio, Prof. Dr. F. Paolucci
Dipartimento di Chimica "G.Ciamician"
Università di Bologna, Via Selmi 2, 40126 Bologna (Italy)
E-mail: francesco.paolucci@unibo.it

[d] Dr. E. R. Kay, Prof. Dr. D. A. Leigh
School of Chemistry, University of Edinburgh
The King's Buildings, West Mains Road
Edinburgh, EH9 3JJ (UK)
E-mail: david.leigh@ed.ac.uk

Supporting information for this article is available on the WWW under http://dx.doi.org/10.1002/chem.201204016.

The observed activation energy and strong solvent polarity effect led us to propose a model in which the displacement of the macrocycle occurs in three stages.[48] First, in the rate-determining step, the hydrogen bonds between the macrocycle and the succinamide station are broken. This occurs more slowly in less-polar solvents. Next, the macrocycle has to move along the thread from the succinamide to the naphthalimide. Molecular dynamics simulations[50] suggest that this can occur on a subnanosecond timescale. In the final stage, the macrocycle binds with the naphthalimide radical anion. The process is reversible, and the position of the ring on the thread is controlled by thermodynamic features. Although the model is attractively simple and in agreement with the available data, its validity needs to be tested. The movement in the second stage can be a random walk along the alkyl chain, which proceeds until the macrocycle is close enough to form a hydrogen bond to one of the stations, whereupon it is "pulled in" irreversibly on the nanosecond timescale. Recently, we showed that the dependence of the shuttling rate on the spacer length could be described very well by a biased random walk model.[48] The origin of the bias, however, was not identified. Therefore, alternative mechanisms need to be considered. If the binding of the macrocycle to the accepting station requires a substantial structural reorganization, this might lead to an energy barrier, which reduces the efficiency of trapping. In experimental observations this will show up as a reduced shuttling rate. Yet another possibility is that the macrocycle stays bound to the initial stations, perhaps with only one hydrogen bond, and is "handed over" from one station to the other. In this case, the whole shuttling process is more like an elementary one-step chemical reaction. The rate can be expected to depend on the geometry and charge distribution of the accepting station, because that binds to the macrocycle in the transition state.

To gain more insight into these questions in the present work, the structure of the original rotaxane **1** was modified. The naphthalimide (NI) was replaced by a naphthalene diimide group (NDI rotaxane **2**), or by a pyromellitimide unit (PMI rotaxane **4**). In the radical anion of the NDI unit, the charge will be more delocalized than in the naphthalimide radical anion. This leads to a weaker binding affinity of the macrocycle to the reduced NDI. In the radical anion of PMI the aromatic unit is smaller, so a larger density of the charge on the carbonyl oxygen atoms can be expected relative to NDI. The relative orientation of the C=O groups of PMI is, however, different, which might have an effect on the binding energy and binding geometry.

If the movement is like a random walk, and if trapping occurs efficiently as soon as a contact between the macrocycle and the accepting station is established, we expect that the shuttling rate will be independent of the nature of the accepting station. We studied the dynamic behavior of these new molecular shuttles with electrochemical and photochemical techniques. It turns out that the rates of shuttling for the naphthalene imide and diimide systems **1** and **2** are similar, but for the pyromellitimide rotaxane **4** it is distinctly lower. This implies that the previous description of the shuttling mechanism needs to be modified.

Results and Discussion

Cyclic voltammetry: As previously demonstrated for rotaxane **1**, cyclic voltammetry (CV) experiments can give useful information about the kinetics and thermodynamics of the shuttling process.[45] Solutions of the naphthalene diimide thread **3** and rotaxane **2** (0.5 mM in THF) displayed the CV curves shown in Figure 1. Both NDI-centered reduction processes are shifted in the case of rotaxane **2** towards less negative potentials with respect to thread **3**, as in the case of NI-rotaxane **1** and the corresponding NI thread. Interestingly, the shift is much larger in the case of the second reduction. For rotaxane **2** and thread **3**, the first reduction potentials are located at $E_{1/2}^{red} = -0.48$ and -0.52 V (versus NHE), respectively, which corresponds to the conversion of the

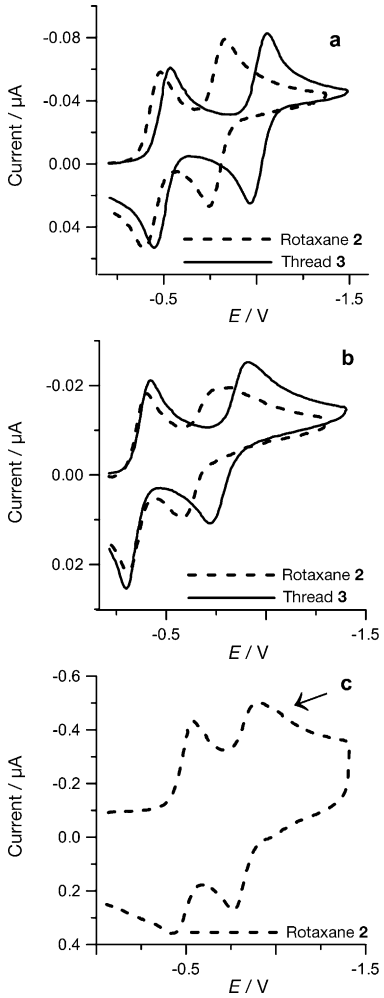

Figure 1. Cyclic voltammograms of rotaxane **2** and thread **3** (0.5 mM in THF, supporting electrolyte: 0.05 M tetrabutylammonium tetrafluoroborate). Working electrode: platinum disc (125 µm diameter). a) $v = 1\ V s^{-1}$ and $T = 25\,°C$; b) $v = 1\ V s^{-1}$, $T = -55\,°C$; c) rotaxane **2**, $v = 100\ V s^{-1}$, $T = 25\,°C$. Reduction potential relative to NHE.

naphthalene diimide to its radical anion (Figure 1a; scan rate (ν) = 1 V s^{-1}). The second reduction potentials are located at $E_{1/2}^{red} = -0.83$ and -1.05 V (versus NHE), for rotaxane **2** and thread **3**, respectively. For thread **3** as well as rotaxane **2**, both reduction processes are essentially reversible (ΔE_p = 80 mV).

The difference in E_p^{red} (I) of the NDI thread and NDI rotaxane is not very large (40 mV), which is similar to that between the mono-imide-thread and rotaxane **1** studied previously, whereas for the second reduction the difference between thread **3** and rotaxane **2** is much bigger (230 mV). The observed shifts are a consequence of the shuttling of the macrocycle from the succinamide station (*succ*-**2** co-conformer), at which it is preferentially located in the neutral state, onto the (reduced) NDI station (*ndi*-**2** co-conformer) and reflect the stabilization of the mono- and dianion of the NDI station as a consequence of their increasing ability to form hydrogen bonds with the macrocycle.

As the scan rate is increased (Figure 1c; ν = 100 V s^{-1}), a small peak is observed (indicated by the arrow in Figure 1c) following the second reduction peak at a potential close to that of the second reduction of **3**. At low temperature, T = -55 °C, ν = 1 V s^{-1}, a broadening of the second peak is observed (Figure 1b; ν = 1 V s^{-1}). The small peak observed in some curves at high scan rate and the broadening at low temperature most likely corresponds to the reduction of $NDI^{\bullet-}$ to NDI^{2-}, whereas the macrocycle still resides on the *succ* station.

As shown before, molecular shuttle **1** in the neutral state adopts the *succ*-**1** co-conformation. ^{1}H NMR spectroscopic evidence shows that the same is true for **2** and **4**. In all cases, the chemical shift of the succinamide methylene protons is $\delta \approx 1.3$ ppm upfield in the rotaxane relative to the corresponding thread. The presence of two succinamide stations in **4** results in signals at both δ = 2.3 and 1.0 ppm, which correspond to the "free" and "occupied" succinamide stations, respectively. Rapid movement of the ring between the succinamide units on either side of the pyromellitimide apparently does not occur. After reduction, the macrocycle shuttles from the succinamide station to the imide unit due to the increased hydrogen-bonding ability of the imides in the reduced state. In the case of $\mathbf{1}^{\bullet-}$, the *ni* co-conformer is strongly favored; but in the case of **2**, a small proportion of the *succ*-$\mathbf{2}^{\bullet-}$ co-conformation seems to be present next to the dominant *ndi*-$\mathbf{2}^{\bullet-}$ co-conformer. A simulation of the CV data (see below) indicates that the ratio *succ*-$\mathbf{2}^{\bullet-}$/*ndi*-$\mathbf{2}^{\bullet-}$ is approximately 1:3. In the doubly reduced state the co-conformational equilibrium strongly favors the *ndi*-$\mathbf{2}^{2-}$ form.

Hydrogen bonding to the macrocycle amide protons stabilizes the increased electron density on the naphthalene diimide, so that more positive potentials must be reached before the oxidation of the dianion occurs, which results in the larger shift observed in the second reoxidation peak. After reoxidation of the dianion, the 1:5 *succ*-$\mathbf{2}^{\bullet-}$/*ndi*-$\mathbf{2}^{\bullet-}$ co-conformational equilibrium is re-established. Further reoxidation of the radical anion regenerates the starting conditions, and the macrocycle moves again to occupy the *succ* binding site most of the time. This behavior can be described by the electrochemical reduction scheme for a redox-switched binding process (Scheme 1). In this scheme, the reversible translational isomerism equilibria for each oxidation state are connected through the electron-transfer steps.[51,52] A computer simulation of all CV results was performed to extract quantitatively the underlying kinetics of the phenomena described above. From these simulations the data compiled in Scheme 1 were obtained as a "best fit".

In all the systems we have investigated so far,[45,53] and in which electron-transfer-induced shuttling was unequivocally observed, the occurrence of shuttling brought about the positive shift of the reduction peak(s) as the result of stabilization of imide-based radical anions by interaction with the macrocycle.

The pyromellitic thread **5** shows two narrowly spaced reversible cathodic peaks at -0.73 and -1.38 V (versus NHE) that correspond to the consecutive one-electron reductions of the pyromellitimide moiety as previously described.[54]

For rotaxane **4** at low scan rates and 25 °C, the first reduction potential is observed at -0.72 V (versus NHE), and the second reduction potential is located at -1.26 V (versus NHE). For thread **5** as well as rotaxane **4**, both reduction processes are essentially reversible (ΔE_p = 80 mV). The reduction potentials of the rotaxanes and threads studied in the present work are listed in Table 1.

Table 1. Reduction potentials [V] of threads **3** and **5** and rotaxanes **2** and **4** relative to NHE.

	Thread **3**	Rotaxane **2**	Thread **5**	Rotaxane **4**
$E_{1/2}^{red}$ (I)	−0.52	−0.48	−0.73	−0.72
$E_{1/2}^{red}$ (II)	−1.05	−0.83	−1.38	−1.26

In summary, the pyromellitic system displays the "typical" electron-transfer-induced shuttling behavior that was observed in all the previous systems. Notice that the apparent $E_{1/2}$ value of CV peaks in the case of square mechanisms such as that shown in Figure 2 depends both on the $E_{1/2}$ values of redox processes that involve the "pure" *succ* and *ndi* co-conformers, respectively, and on the relative values of equilibrium constants that involve the two co-conformers in the oxidized and reduced states, respectively. The negligible shift of the first reduction peak in the rotaxane with respect to the thread does not necessarily imply that shuttling does not occur at the level of first reduction, rather it is indicative that, also after reduction, the equilibrium is in that case only slightly shifted toward the *ndi* co-conformer. In line with this explanation, the much larger positive shift (120 mV) observed at the level of the second reduction peak of rotaxane **4** with respect to thread **5** is associated with the much larger displacement of equilibrium between the two co-conformers upon the introduction of a second electron in the pyromellitic unit.

Spectroelectrochemistry: Further evidence for shuttling in rotaxanes **2** and **4** was found with UV-visible spectroelectro-

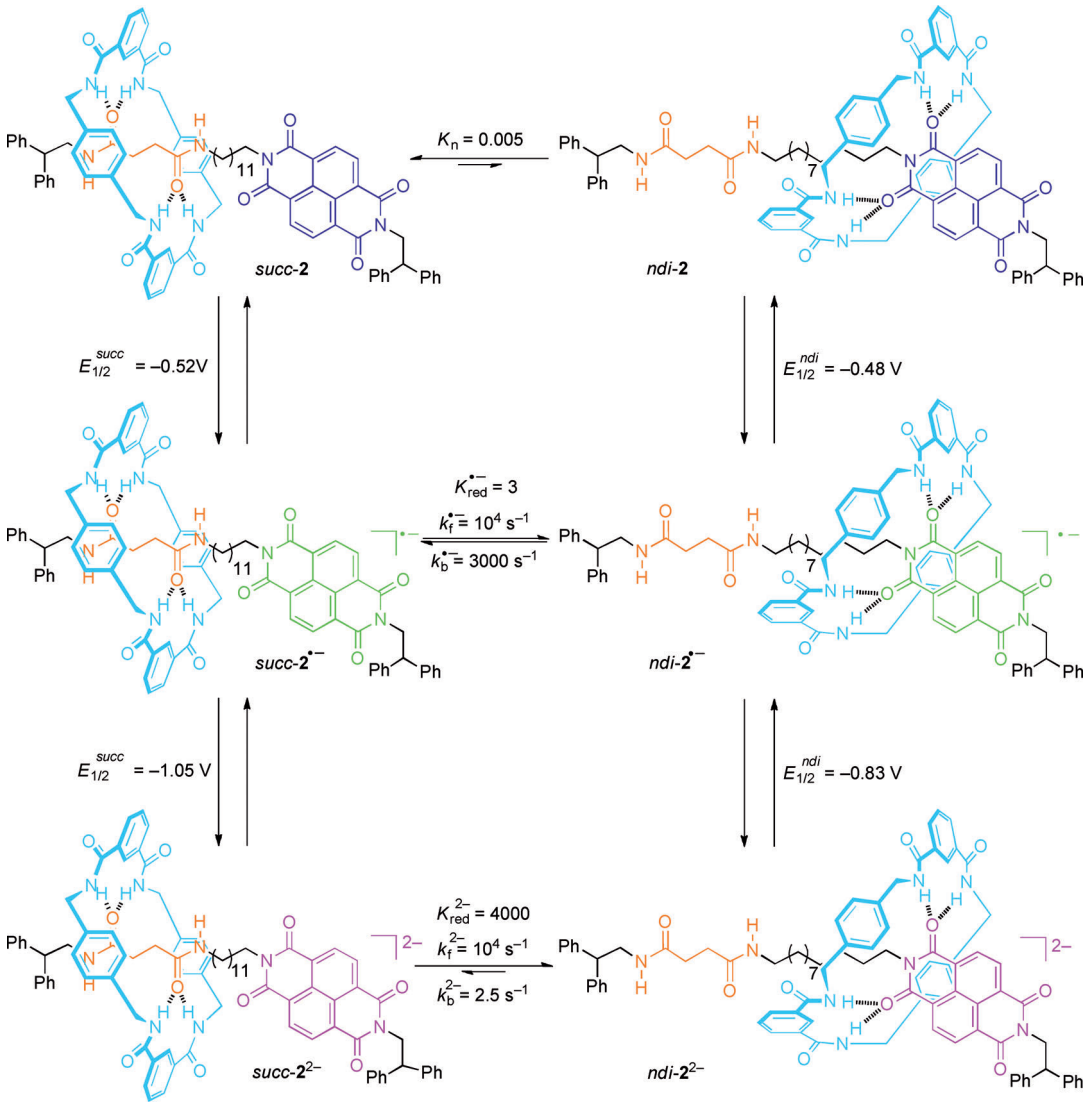

Scheme 1. Electrochemical reduction cycle of rotaxane **2** and equilibrium constants obtained from simulation of the CV curves.

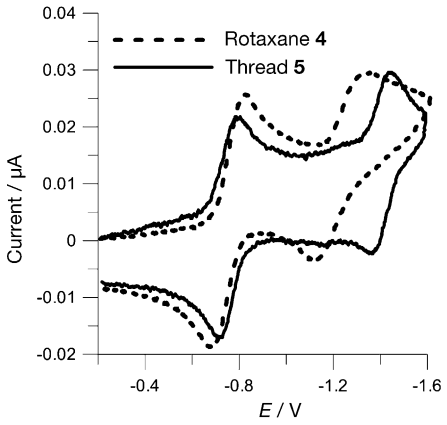

Figure 2. Cyclic voltammograms of rotaxane **4** and thread **5** (0.5 mM in THF, supporting electrolyte: 0.05 M tetrabutylammonium tetrafluoroborate). Working electrode: platinum disc (125 µm diameter); v = 1 V s^{-1} and T = 25 °C. Reduction potentials relative to NHE.

chemistry. In the case of naphthalimide rotaxane **1**, several of the radical anion absorption bands were found to occur at shorter wavelengths than those of the corresponding thread.[49] These blueshifts occur because the hydrogen bonds between the macrocycle and the carbonyls of the imide stabilize the ground state of the anion more than its excited state. The spectra of naphthalene diimide thread **3** and rotaxane **2** and their radical anions and dianions, depicted in Figure 3, show similar behavior. The spectra of the neutral thread **3** and rotaxane **2** are identical, which is in agreement with binding of the macrocycle to the succinamide in the neutral form. Upon reduction, the typical spectra for the naphthalene diimide radical anion and dianion are observed.[55] Although the spectra of the reduced forms of **2** and **3** are similar, some clear peak shifts can be seen. The absorption maxima and molar absorption coefficients are listed in Table 2.

The low-energy absorption maxima of the radical anion and the dianion of rotaxane **2** are shifted to shorter wave-

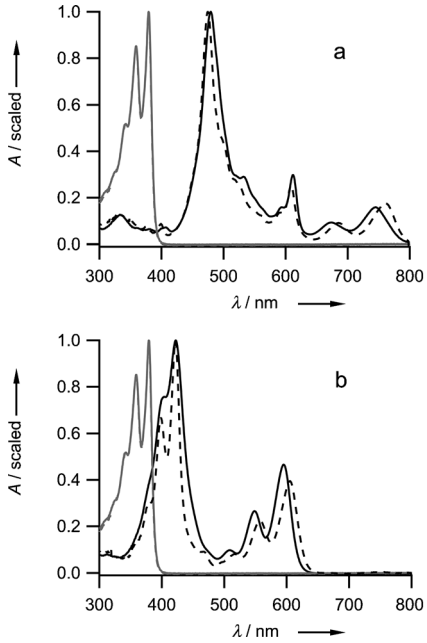

Figure 3. The absorption spectra of a) the radical anion and b) the dianion of naphthalene diimide rotaxane **2** (solid line), and thread **3** (dashed line) in THF. The spectra of the neutral molecules (identical for **2** and **3**) are shown in gray.

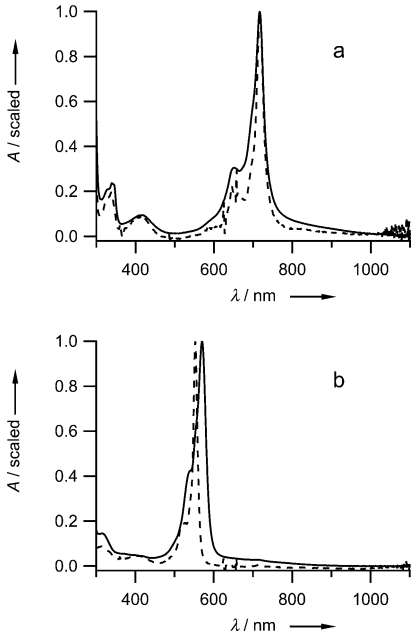

Figure 4. Normalized absorption spectra of a) the pyromellitic radical anion and b) dianion of the thread **5** (dashed line) and rotaxane **4** (solid line) in THF.

Table 2. Absorption maxima (wavelength λ [nm] and molar absorption coefficients ε [$10^3\,\text{M}^{-1}\,\text{cm}^{-1}$]) of the radical anions and dianions of thread **3** and rotaxane **2**.

	λ_1 (ε_1)	λ_2 (ε_2)	λ_3 (ε_3)	λ_4 (ε_4)	λ_5 (ε_5)
$\mathbf{3}^{\bullet-}$	474 (30)	609 (7.4)	684 (2.5)	763 (5.0)	
$\mathbf{2}^{\bullet-}$	479 (27)	612 (8.0)	674 (2.5)	745 (4.2)	
$\mathbf{3}^{2-}$	399 (16)	422 (24)	516 (4.8)	557 (6.5)	605 (11)
$\mathbf{2}^{2-}$	402 (19)	422 (26)	509 (2.5)	548 (6.8)	595 (12)

lengths than those of thread **3**. These shifts indicate the translocation of the macrocycle from the succinamide to the naphthalene diimide stations in the reduced form. The absorption bands at 674 and 745 nm of the rotaxane radical anion are somewhat broader than those of the thread, probably because of the presence of a small fraction of the *succ*-$\mathbf{2}^{\bullet-}$ co-conformer, which is in agreement with the CV results.

The absorption spectra of the radical anions and dianions of the pyromellitimide thread **5** and rotaxane **4** in tetrahydrofuran (THF) are depicted in Figure 4. The absorption maxima are listed in Table 3. The spectra are similar to previously reported spectra of anions of pyromellitic diimides.[55–57] The radical anion spectra of thread **5** and rotaxane **4** are very similar, with a strong absorption at 716 nm.

Table 3. Absorption maxima of the pyromellitic radical anion and dianion of thread **5** and rotaxane **4**.

	Radical anion [nm]	Dianion [nm]
thread **5**	717	553
rotaxane **4**	716	570

The molar absorption coefficient of the similar *N,N'*-bis(2,5-di-*tert*-butylphenyl) pyromellitic imide radical anion is $4.17\times10^4\,\text{M}^{-1}\,\text{cm}^{-1}$ according to Rak et al.[56] On the basis of this value, the molar absorption coefficient of the dianion is estimated to be approximately $1.1\times10^5\,\text{M}^{-1}\,\text{cm}^{-1}$. This is slightly lower than the value ($1.4\times10^5\,\text{M}^{-1}\,\text{cm}^{-1}$) measured by Gosztola et al.[55]

The spectrum of the radical anion of rotaxane **4** is only slightly blueshifted at the peak, but broadened and more intense in the short-wavelength shoulder relative to that of thread **5**. The change in shape indicates that there is an interaction between the macrocyclic ring and the chromophore, which means that in the radical anion there must be a significant population of the *pmi*-$\mathbf{4}^{\bullet-}$ co-conformer. Molecular computation (see below) indicates that the macrocyclic ring binds more strongly to the $\text{PMI}^{\bullet-}$ than to $\text{NDI}^{\bullet-}$. Further independent evidence for essentially complete translocation of the macrocycle from infrared spectroelectrochemistry will be published elsewhere.[58]

In the dianions, the absorption maximum of the rotaxane is broadened and distinctly redshifted by 17 nm. The redshift is in contrast with the blueshifts observed in the cases of the naphthalene mono and diimide radical anions and NDI dianion, but the spectral changes in combination with the result for the radical anion leave no doubt that the predominant co-conformer is *pmi*-$\mathbf{4}^{2-}$.

Note that although the pyromellitimide rotaxane **4** has two equivalent succinamide stations, only one of them is involved in the shuttling process. The ^{1}H NMR spectra (see the Supporting Information) show that the macrocyclic ring is localized on one of the succinamide stations, and shuttling

between the two equivalent sites is not detectable on the NMR spectroscopic timescale.

Computation: To test our intuitive expectations of the relative binding strengths of the macrocyclic ring to the different stations, some ab-initio calculations were performed. Owing to the size and complexity of the systems we had to restrict ourselves to the B3LYP/6-31G(d) level of calculation on selected model systems. Calculations were performed for isolated molecules and for molecules solvated in acetonitrile with the polarizable continuum model (PCM).[59,60] The geometries of the isolated molecules were used.

Two conformations were considered for the macrocyclic ring: a chair (C_{2h}) and a boat (C_{2v} symmetry). For the free macrocycle, the latter turned out to be lower in energy by 1 kcal mol^{-1}. The succinamide thread unit was modeled with the full diphenylethyl stopper on one side and a methyl group mimicking the alkane linker. For the isolated molecules, the thread model was most stable in a conformation with an intramolecular hydrogen bond, but when solvated, the extended conformation was preferred. The imides were in all cases modeled as the NH derivatives. To estimate the relative interaction energies, a complex of the succinamide model with the chair macrocycle was compared with the complexes of the boat macrocycle with the imides (C_{2v} symmetry). Model structures are shown in Figure S3 in the Supporting Information. In Table 4 we list the differences in the

Table 4. Computed binding energies (B3LYP/6-31G(d) [kcal mol^{-1}]) of the tetralactam macrocycle to imides in neutral, radical anion, and dianion states, relative to binding to a succinamide model. Structures are shown in the Supporting Information.

	NI	NI (CH_3CN)[a]	NDI	NDI (CH_3CN)[a]	PMI	PMI (CH_3CN)[a]
neutral	4.4	1.4	7.0	2.4	8.0	3.7
anion	−26.7	−9.2	−17.1	−3.8	−18.9	−6.3
dianion			−55.1	−12.0	−65.1	

[a] Polarizable continuum model for acetonitrile, with gas-phase geometries.

binding energies of the macrocyclic ring with the imide model and with the thread model. For the neutral molecules these values are all positive, which means that the ring prefers to bind to the succinamide; for the radical anions and dianions they are negative. This means that overall the results are in agreement with our experimental findings. More details are given in the Supporting Information.

Of the three radical anions, the naphthalene diimide is computed to have the least favorable interaction with the macrocycle. This agrees qualitatively with our observation that the equilibrium constant of the *ndi*-**2**$^{\bullet-}$/*succ*-**2**$^{\bullet-}$ equilibrium is only about 5. The pyromellitimide anion is predicted to bind more strongly to the macrocycle. On the basis of this result and those of the IR study,[58] it is reasonable to assume that in the case of **4**$^{\bullet-}$ the co-conformational equilibrium favors the *pmi*-**4**$^{\bullet-}$ co-conformer.

Photoreduction: In the case of the naphthalimide rotaxane **1**, photoinduced electron transfer was used to generate the radical anion, and the shift in the position of the absorption was used to monitor the shuttling process in time with transient-absorption spectroscopy on a microsecond timescale. Charge recombination restores the neutral ground-state form of the system, so that no net chemical change occurs and repeated excitation of the sample can be used. Unfortunately, direct excitation of naphthalene diimides resulted in rapid photodegradation.[61–63] Also, in the presence of 1,4-diaza[2.2.2]bicyclooctane (DABCO) as an electron donor, reversible formation of radical anions could not be achieved. To avoid the reactive excited state of the naphthalene diimide, excitation of 1,4-dimethoxybenzene (DMB), an electron donor, in the presence of naphthalene diimide was used as an alternative route to the radical anion. Benzonitrile was used as the solvent. To investigate the mechanism, we used naphthalene diimide model compound **6**. Excitation of DMB with a 310 nm laser pulse in the presence of naphthalene diimide **6** in benzonitrile gave a transient-absorption spectrum (Figure 5) that resembles the naphthalene diimide radical anion spectrum well (Figure 3).

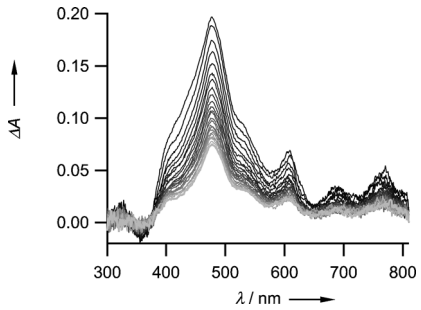

Figure 5. Transient-absorption spectra of a 100 μM solution of **6** in benzonitrile after excitation of DMB (20 mM) with 310 nm (the highest ΔA was at 2 μs after the laser pulse, subsequent spectra at later times, with an increment of 2 μs).

The driving force for electron transfer in polar solvents can be calculated from Equation (1), in which ΔG is the free energy change, eE_{ox} and eE_{red} are the relative energies of the oxidized electron donor and reduced electron acceptor, and E_{00} is the electronic excitation energy.

$$\Delta G = eE_{ox} - eE_{red} - E_{00} \quad (1)$$

The excitation energy of DMB in the S_1 state is 4.0 eV, and its oxidation potential is 1.58 V (versus NHE).[64] The driving force for electron transfer between DMB and naphthalene diimides ($E_{red} = -0.24$ V versus NHE)[55] can be estimated as −2.2 eV. Electron transfer between DMB and benzonitrile ($E_{red} = -1.98$ V versus NHE)[65] has a driving force of −0.4 eV. The formation of NDI radical anions can take place directly by reaction of the diimide with excited DMB, but since the concentration of the diimide is only approximately 10^{-4} M, this is kinetically unlikely during the nanosec-

ond lifetime of the DMB excited singlet state. Alternatively, the benzonitrile radical anion could be formed first, followed by electron transfer to NDI. Electron transfer between DMB in the S_1 state and acceptors with reduction potentials in the same range as benzonitrile has been observed before.[66] To distinguish between the two pathways, the fluorescence and transient absorption of DMB in acetonitrile and benzonitrile were studied.

Time-resolved fluor escence of DMB ($\lambda_{ex}=310$ nm) in acetonitrile and benzonitrile was measured by using a streak camera. The fluorescence spectra (Figure 6) ($\lambda_{max}=328$ nm) and lifetime of 2.7 ns observed in degassed acetonitrile are

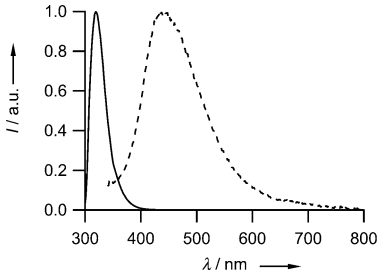

Figure 6. Fluorescence spectra of DMB in acetonitrile (solid line) and benzonitrile (dashed line).

in good agreement with literature data for DMB.[67] In benzonitrile the fluorescence has a maximum around 450 nm and a biexponential decay with lifetimes of 3.5 and 9.6 ns. Between 300 and 400 nm, there is weak shoulder with a lifetime of 2.3 ns. The changes in the fluorescence spectrum and the longer lifetimes indicate the formation of an exciplex between DMB and benzonitrile.

The transient-absorption spectra of DMB in degassed acetonitrile and benzonitrile are depicted in Figure 7. The spectra in acetonitrile have a maximum around 425 nm, decay in 10 μs, and correspond with the known triplet–triplet absorption spectra of dimethoxybenzene.[68] The assignment to the triplet is supported by the fact that in the presence of air the decay becomes much faster (100 ns) due to quenching by oxygen. The spectra observed in benzonitrile resemble more the summed spectra of the radical cation of DMB[68–70] and the radical anion of benzonitrile.[71,72] The decay of the transient in benzonitrile is not sensitive to oxygen, thus indicating that the observed band is mainly due to the DMB radical cation. Moreover, the decay follows second-order kinetics, as expected for separated radical ion pairs in solution. The observed exciplex fluorescence in benzonitrile and the differences in transient-absorption dynamics strongly suggest that electron transfer between DMB and the solvent benzonitrile occurs, followed by reduction of the diimide by the benzonitrile radical anion.

Shuttling: When the radical anion of rotaxane **2** is created by laser-induced electron transfer, the spectral evolution can be monitored in time with transient-absorption spectroscopy. Figure 8 shows an image of the transient-absorption

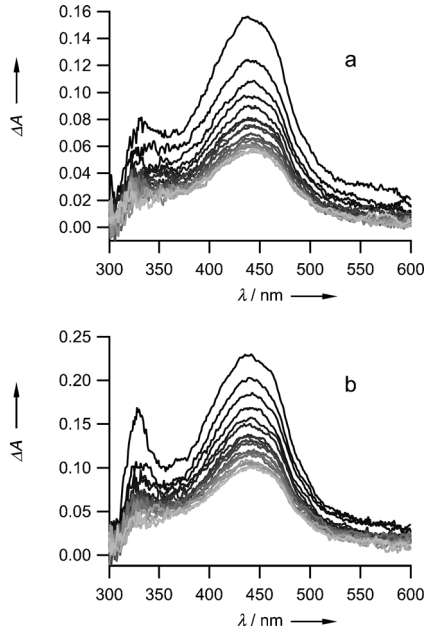

Figure 7. Transient-absorption spectra of DMB in a) acetonitrile and b) benzonitrile; $\lambda_{ex}=315$ nm. Time increments between successive spectra 1 μs.

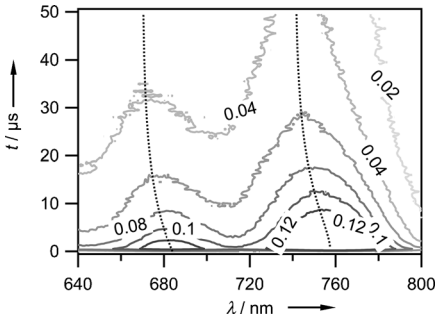

Figure 8. Contour plot of the transient-absorption spectra in benzonitrile. The dotted lines show the shift of the maxima.

spectra of a solution of rotaxane **2** and dimethoxybenzene in benzonitrile after excitation with a nanosecond laser pulse at 315 nm. At short times, the radical anion absorption bands are those of the *succ*-**2**$^{\bullet-}$ co-conformer, very similar to those of thread **3**$^{\bullet-}$ observed in the spectroelectrochemical experiments. On a timescale of tens of microseconds, the spectrum evolves into the blueshifted one of the *ndi*-**2**$^{\bullet-}$ co-conformer.

The same experiment with thread **3** instead of rotaxane **2** did not show such a shift. This behavior corresponds to that of the previously described naphthalimide shuttle **1**.

To obtain the shuttling rate constant, the spectral evolution was quantitatively modeled. The two absorption bands in the spectra of the radical anions of the thread and rotaxane between 650 and 800 nm were fitted as a linear combination of two Gaussian functions (see Figure S2 and Table S1 in the Supporting Information). The similar band

shapes found for the initial and final states suggest that the population of the *succ* co-conformer in the radical anion in benzonitrile is smaller than in THF, in which the electrochemical experiments were carried out (see Figure 3). Then, the obtained transient-absorption spectra at different times were fitted as a superposition of those two functions. From the obtained amplitude for each spectrum the relative contributions were calculated (Figure 9). The change of the relative contribution of each spectrum corresponds to the change in population of each species.

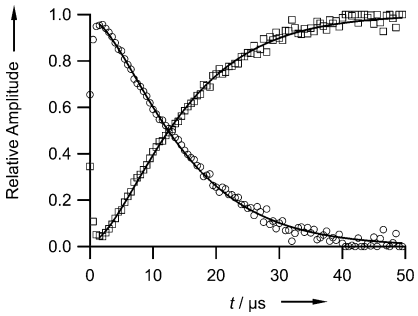

Figure 9. Change of the fractions of the *succ*-$\mathbf{2}^{\bullet-}$ co-conformer (circles) and *ndi*-$\mathbf{2}^{\bullet-}$ co-conformer (squares) with time. The curves are fits with a biexponential model.

The change in population of the two co-conformers of $\mathbf{2}^{\bullet-}$ shows an exponential time profile, with a time constant of 13 μs. In the case of establishment of an equilibrium following a perturbation, the observed rate constant is the sum of the forward and backward rate constants, but if we neglect the equilibrium population of the *succ* co-conformer in the radical anion state, the obtained $8\times10^5\,s^{-1}$ is just the forward shuttling rate constant. At shorter times there is a relatively slow rise that was modeled with an additional exponential. This is probably caused by the fact that it takes a few microseconds to form the NDI radical anion. So in the first five microseconds there is the formation of the radical anion and also shuttling of the already formed radical anions.

The shuttling time constant of rotaxane **1** in benzonitrile was measured in the same way as before,[49] and found to be 10 μs.

Photoreduction of the pyromellitic diimide thread **5** was attempted by using the same procedure used for reduction of the naphthalene diimide thread and rotaxane. Excitation at 315 nm of a 20 mM dimethoxybenzene solution with 10^{-4} M PMI thread **5** gave the transient-absorption spectra shown in Figure 10.

Two main peaks are present: one at 723 nm with a shoulder at 659 nm that corresponds to the radical anion spectrum shown in Figure 4. The other band has a maximum at 437 nm. This is due to the dimethoxybenzene radical cation spectrum (compare with Figure 7). This shows that it is possible to create the pyromellitic radical anion photochemically by excitation of the dimethoxybenzene electron donor.

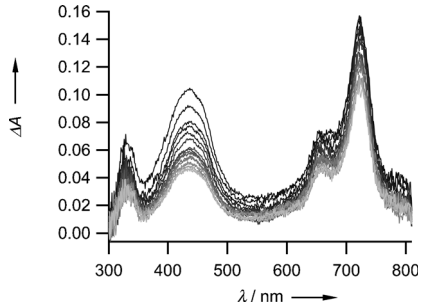

Figure 10. Transient-absorption spectra of 122 μM PMI thread **5** in benzonitrile after excitation of DMB (6 mM) with a 315 nm laser pulse. The first spectrum is 6 μs after the pulse. The consecutive spectra (black to gray) were measured with a time increment of 2 μs.

The radical anion transient-absorption bands of the PMI rotaxane **4** were analyzed in the same way as for rotaxane **2**. The analysis gave a time constant of 44 μs (Figure 11). Although the accuracy is not deemed very high because of the relatively small spectral changes, the shuttling process in $\mathbf{4}^{-}$ is clearly slower than that in $\mathbf{2}^{-}$ and $\mathbf{1}^{-}$.

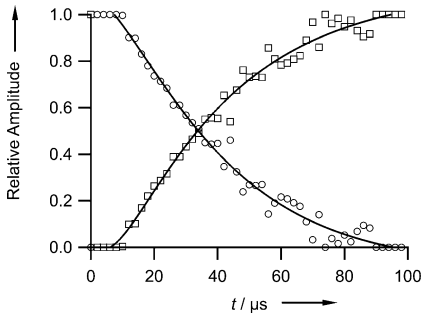

Figure 11. The relative amplitude of the initial (circles) and final (squares) spectrum of the radical anions of the PMI [2]rotaxane **4** in time.

In our initial paper on the shuttling in naphthalimide rotaxane **1**, we observed that the rate of the process increased strongly as solvent polarity increased, and we determined a free energy of activation of 10 kcal mol^{-1}, which we considered to indicate that in the transition state of the reaction, hydrogen bonds to the initial binding station were broken.[49] The shuttling would then continue with a diffusive random walk of the ring along the thread, thus leading to its trapping by the accepting naphthalimide anion station. Somewhat puzzling was the negative entropy of activation, but this can be attributed to the probability factor ($P<1$) involved in the second stage of the reaction. More recently, the dependence of the rate of the length of the spacer between the binding sites was found to be in agreement with a biased random walk.[48] In this model, the accepting station has a passive role, and the strength of its interactions with the macrocycle has no influence on the reaction rate. The present findings with pyromellitimide rotaxane **4**, however, indicate that the rate does depend on the nature of the ac-

cepting station. Because the hydrocarbon linkers between the stations are flexible, an alternative mechanism might be considered in which the shuttling proceeds in one kinetic step through a transition state in which the macrocyclic ring is bound to both stations, while the flexible spacer is folded. A sketch of one of many possible transition structures is shown in Figure 12.

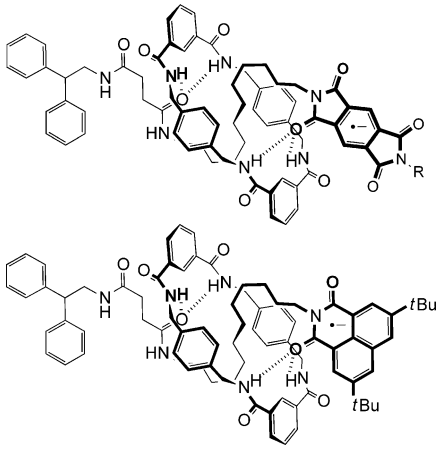

Figure 12. Examples of possible "harpooning" transition structures for shuttling in $\mathbf{4}^{\bullet-}$ and $\mathbf{1}^{\bullet-}$.

Such a "harpooning" mechanism is qualitatively compatible with the observed distance dependence, because formation of the transition-state structure is statistically less likely as the length of the spacer is increased. Conformations in which the tetralactam ring is hydrogen-bonded to two stations have been observed in crystal structures, and have even been proposed as preferred energy minima in particular in cases in which the binding to the stations is relatively weak.[73] Infrared absorption[46] and NMR spectroscopic studies, and X-ray crystallography[73] have also provided evidence for the existence of "bridged" conformations in hydrogen-bond-based rotaxanes.[74] Although in this harpooning mechanism the ring is always hydrogen-bonded to a station, the number of hydrogen bonds in the transition state is smaller than in the initial state, so our initial explanation of the solvent effect still holds. Finally, the negative entropies of activation are readily explained by this mechanism because in the transition state many degrees of freedom are more or less frozen.

Whereas the available experimental data show that a passive mechanism in which the acceptor station has no role in determining the shuttling rate is not correct for the compounds studied in the present work, the generality of this observation remains to be investigated. Rotaxanes of the type discussed in the present paper can be designed in such a way that harpooning can be excluded by incorporating a sufficiently long rigid thread unit. Unfortunately, such systems are difficult to obtain experimentally because of solubility problems.[74]

For the other classes of rotaxane molecular shuttles described in the literature, it seems to be tacitly assumed that the ring slides along the thread in a diffusive process.[75–77] With very few exceptions, the threads are highly flexible,[78] and therefore we suggest that in many cases harpooning-type mechanisms should be considered as alternatives. In one case, it was reported that electrostatically induced folding actually prevented shuttling.[79] In highly viscous or otherwise constrained environments, such as polymer gels, large-amplitude motions are restricted.[80] In such a situation, the different steric requirements of diffusive and harpooning mechanisms might be important. For example, if the stoppers are much larger than the moving ring, the contraction of the thread that is required for harpooning might be hindered more than the diffusive motion of the ring.

Conclusion

New rotaxanes were synthesized that incorporated different diimides as redox-active stations and succinamide as a common template for ring formation and the preferred binding site in the neutral molecules. ^{1}H NMR spectroscopy of naphthalene diimide rotaxane **2** and pyromellitic diimide rotaxane **4** demonstrated that the tetralactam macrocycle binds exclusively to the succinamide station in the neutral molecules. Thermodynamic data derived from cyclic voltammetry of **2** showed that the macrocycle binds predominantly to the diimide in the radical anion state, and exclusively to the diimide in the dianion. Spectral changes upon shuttling were observed by UV-visible spectroelectrochemistry and in time-resolved experiments in which reduction was achieved by laser-induced photochemistry. The rate of the shuttling process at room temperature in benzonitrile was found to be 8×10^5 s^{-1}, which is only slightly slower than that in rotaxane **1**, for which it is 1×10^6 s^{-1}.

The smaller strength of binding in the naphthalene diimide does not have a significant effect on the rate, which is consistent with our original hypothesis that the rate-limiting step in the shuttling process is the release of the macrocycle from its initial succinamide binding station. The results with the pyromellitimide rotaxane **4**, however, shed doubt on this mechanism, because in this case the rate is approximately three times smaller. As an alternative to the two-step mechanism, a single-step harpooning process should be considered.

Experimental Section

Experimental details are given in the Supporting Information.

Acknowledgements

This research was financially supported by the Netherlands Organization for the Advancement of Research (NWO). Berta Garcia-Landa made a crucial contribution to the frontispiece illustration.

[1] *Molecular Motors* (Ed.: M. Schliwa), Wiley VCH, Weinheim, **2003**.
[2] V. Bormuth, V. Varga, J. Howard, E. Schaffer, *Science* **2009**, *325*, 870–873.
[3] A. Yildiz, M. Tomishige, R. D. Vale, P. R. Selvin, *Science* **2004**, *303*, 676–678.
[4] R. D. Vale, R. A. Milligan, *Science* **2000**, *288*, 88–95.
[5] Z. Zhang, D. Thirumalai, *Structure* **2012**, *20*, 628–640.
[6] W. B. Redwine, R. Hernández-López, S. Zou, J. Huang, S. L. Reck-Peterson, A. E. Leschziner, *Science* **2012**, *337*, 1532–1536.
[7] N. D. Derr, B. S. Goodman, R. Jungmann, A. E. Leschziner, W. M. Shih, S. L. Reck-Peterson, *Science* **2012**, *338*, 662–665.
[8] E. R. Kay, D. A. Leigh, F. Zerbetto, *Angew. Chem.* **2007**, *119*, 72–196; *Angew. Chem. Int. Ed.* **2007**, *46*, 72–191.
[9] T. Kudernac, N. Ruangsupapichat, M. Parschau, B. Macia, N. Katsonis, S. R. Harutyunyan, K.-H. Ernst, B. L. Feringa, *Nature* **2011**, *479*, 208–211.
[10] G. T. Carroll, M. M. Pollard, R. van Delden, B. L. Feringa, *Chem. Sci.* **2010**, *1*, 97–101.
[11] B. L. Feringa, *J. Org. Chem.* **2007**, *72*, 6635–6652.
[12] W. R. Browne, B. L. Feringa, *Nat. Nanotechnol.* **2006**, *1*, 25–35.
[13] Y.-C. You, M.-C. Tzeng, C.-C. Lai, S.-H. Chiu, *Org. Lett.* **2012**, *14*, 1046–1049.
[14] C. J. Chuang, W. S. Li, C. C. Lai, Y. H. Liu, S. M. Peng, I. Chao, S. H. Chiu, *Org. Lett.* **2009**, *11*, 385–388.
[15] K. Hirose, Y. Shiba, K. Ishibashi, Y. Doi, Y. Tobe, *Chem. Eur. J.* **2008**, *14*, 3427–3433.
[16] T. Umehara, H. Kawai, K. Fujiwara, T. Suzuki, *J. Am. Chem. Soc.* **2008**, *130*, 13981–13988.
[17] S. Silvi, M. Venturi, A. Credi, *Chem. Commun.* **2011**, *47*, 2483–2489.
[18] T. Avellini, H. Li, A. Coskun, G. Barin, A. Trabolsi, A. N. Basuray, S. K. Dey, A. Credi, S. Silvi, J. F. Stoddart, *Angew. Chem.* **2012**, *124*, 1643–1647; *Angew. Chem. Int. Ed.* **2012**, *51*, 1611–1615.
[19] S. Saha, J. F. Stoddart, *Chem. Soc. Rev.* **2007**, *36*, 77–92.
[20] R. E. Dawson, S. F. Lincoln, C. J. Easton, *Chem. Commun.* **2008**, 3980–3982.
[21] P. Raiteri, G. Bussi, C. S. Cucinotta, A. Credi, J. F. Stoddart, M. Parrinello, *Angew. Chem.* **2008**, *120*, 3592–3595; *Angew. Chem. Int. Ed.* **2008**, *47*, 3536–3539.
[22] J. Wang, B. L. Feringa, *Science* **2011**, *331*, 1429–1432.
[23] A. Coskun, M. Banaszak, R. D. Astumian, J. F. Stoddart, B. A. Grzybowski, *Chem. Soc. Rev.* **2012**, *41*, 19–30.
[24] M. von Delius, E. M. Geertsema, D. A. Leigh, D. T. D. Tang, *J. Am. Chem. Soc.* **2010**, *132*, 16134–16145.
[25] M. J. Barrell, A. G. Campaña, M. von Delius, E. M. Geertsema, D. A. Leigh, *Angew. Chem.* **2011**, *123*, 299–304; *Angew. Chem. Int. Ed.* **2011**, *50*, 285–290.
[26] A. G. Campaña, A. Carlone, K. Chen, D. T. F. Dryden, D. A. Leigh, U. Lewandowska, K. M. Mullen, *Angew. Chem.* **2012**, *124*, 5576–5579; *Angew. Chem. Int. Ed.* **2012**, *51*, 5480–5483.
[27] P. Kovaříček, J.-M. Lehn, *J. Am. Chem. Soc.* **2012**, *134*, 9446–9455.
[28] S. A. Vignon, T. Jarrosson, T. Iijima, H.-R. Tseng, J. K. M. Sanders, J. F. Stoddart, *J. Am. Chem. Soc.* **2004**, *126*, 9884–9885.
[29] T. Iijima, S. A. Vignon, H. R. Tseng, T. Jarrosson, J. K. M. Sanders, F. Marchioni, M. Venturi, E. Apostoli, V. Balzani, J. F. Stoddart, *Chem. Eur. J.* **2004**, *10*, 6375–6392.
[30] K. M. Mullen, K. D. Johnstone, M. Webb, N. Bampos, J. K. M. Sanders, M. J. Gunter, *Org. Biomol. Chem.* **2008**, *6*, 278–286.
[31] Y. Makita, N. Kihara, T. Takata, *J. Org. Chem.* **2008**, *73*, 9245–9250.
[32] V. Balzani, A. Credi, M. Venturi, *Chem. Soc. Rev.* **2009**, *38*, 1542–1550.
[33] A. Moretto, I. Menegazzo, M. Crisma, E. J. Shotton, H. Nowell, S. Mammi, C. Toniolo, *Angew. Chem.* **2009**, *121*, 9148–9151; *Angew. Chem. Int. Ed.* **2009**, *48*, 8986–8989.
[34] F. Durola, J. Lux, J.-P. Sauvage, *Chem. Eur. J.* **2009**, *15*, 4124–4134.
[35] I. Murgu, J. M. Baumes, J. Eberhard, J. J. Gassensmith, E. Arunkumar, B. D. Smith, *J. Org. Chem.* **2011**, *76*, 688–691.
[36] J. M. Baumes, I. Murgu, A. Oliver, B. D. Smith, *Org. Lett.* **2010**, *12*, 4980–4983.
[37] P. Lussis, T. Svaldo-Lanero, A. Bertocco, C. A. Fustin, D. A. Leigh, A. S. Duwez, *Nat. Nanotechnol.* **2011**, *6*, 553–557.
[38] D. D. Günbaş, L. Zalewski, A. M. Brouwer, *Chem. Commun.* **2011**, *47*, 4977–4979.
[39] T. Ogoshi, D. Yamafuji, T. Aoki, T. Yamagishi, *J. Org. Chem.* **2011**, *76*, 9497–9503.
[40] T. Ogoshi, D. Yamafuji, T. Aoki, K. Kitajima, T.-A. Yamagishi, Y. Hayashi, S. Kawauchi, *Chem. Eur. J.* **2012**, *18*, 7493–7500.
[41] T. Ogoshi, D. Yamafuji, T. Aoki, T.-A. Yamagishi, *Chem. Commun.* **2012**, *48*, 6842–6844.
[42] S. W. Hansen, P. C. Stein, A. Sørensen, A. I. Share, E. H. Witlicki, J. Kongsted, A. H. Flood, J. O. Jeppesen, *J. Am. Chem. Soc.* **2012**, *134*, 3857–3863.
[43] A. Joosten, Y. Trolez, J.-P. Collin, V. Heitz, J.-P. Sauvage, *J. Am. Chem. Soc.* **2012**, *134*, 1802–1809.
[44] H. Li, A. C. Fahrenbach, A. Coskun, Z. Zhu, G. Barin, Y.-L. Zhao, Y. Y. Botros, J.-P. Sauvage, J. F. Stoddart, *Angew. Chem.* **2011**, *123*, 6914–6920; *Angew. Chem. Int. Ed.* **2011**, *50*, 6782–6788.
[45] A. Altieri, F. G. Gatti, E. R. Kay, D. A. Leigh, D. Martel, F. Paolucci, A. M. Z. Slawin, J. K. Y. Wong, *J. Am. Chem. Soc.* **2003**, *125*, 8644–8654.
[46] D. C. Jagesar, F. Hartl, W. J. Buma, A. M. Brouwer, *Chem. Eur. J.* **2008**, *14*, 1935–1946.
[47] M. R. Panman, P. Bodis, D. J. Shaw, B. H. Bakker, A. C. Newton, E. R. Kay, D. A. Leigh, W. J. Buma, A. M. Brouwer, S. Woutersen, *Phys. Chem. Chem. Phys.* **2012**, *14*, 1865–1875.
[48] M. R. Panman, P. Bodis, D. J. Shaw, B. H. Bakker, A. C. Newton, E. R. Kay, A. M. Brouwer, W. J. Buma, D. A. Leigh, S. Woutersen, *Science* **2010**, *328*, 1255–1258.
[49] A. M. Brouwer, C. Frochot, F. G. Gatti, D. A. Leigh, L. Mottier, F. Paolucci, S. Roffia, G. W. H. Wurpel, *Science* **2001**, *291*, 2124–2128.
[50] M. Socol, P. D. Zoon, A. M. Brouwer, unpublished results.
[51] M. von Delius, E. M. Geertsema, D. A. Leigh, *Nat. Chem.* **2010**, *2*, 96–101.
[52] S. A. Lerke, D. H. Evans, S. W. Feldberg, *J. Electroanal. Chem. Interfacial Electrochem.* **1990**, *296*, 299–315.
[53] G. Fioravanti, N. Haraszkiewicz, E. R. Kay, S. M. Mendoza, C. Bruno, M. Marcaccio, P. G. Wiering, F. Paolucci, P. Rudolf, A. M. Brouwer, *J. Am. Chem. Soc.* **2008**, *130*, 2593–2601.
[54] A. Viehbeck, M. J. Goldberg, C. A. Kovac, *J. Electrochem. Soc.* **1990**, *137*, 1460–1466.
[55] D. Gosztola, M. P. Niemczyk, W. Svec, A. S. Lukas, M. R. Wasielewski, *J. Phys. Chem. A* **2000**, *104*, 6545–6551.
[56] S. F. Rak, T. H. Jozefiak, L. L. Miller, *J. Org. Chem.* **1990**, *55*, 4794–4801.
[57] S. L. Buchwalter, R. Iyengar, A. Viehbeck, T. R. O'Toole, *J. Am. Chem. Soc.* **1991**, *113*, 376–377.
[58] D. C. Jagesar, J. Baggerman, P. G. Wiering, E. Kay, D. A. Leigh, A. M. Brouwer, unpublished results.
[59] Gaussian 03 (Revision B.03), M. J. Frisch, G. W. Trucks, H. B. Schlegel, G. E. Scuseria, M. A. Robb, J. R. Cheeseman, J. A. Montgomery, Jr., T. Vreven, K. N. Kudin, J. C. Burant, J. M. Millam, S. S. Iyengar, J. Tomasi, V. Barone, B. Mennucci, M. Cossi, G. Scalmani, N. Rega, G. A. Petersson, H. Nakatsuji, M. Hada, M. Ehara, K. Toyota, R. Fukuda, J. Hasegawa, M. Ishida, T. Nakajima, Y. Honda, O. Kitao, H. Nakai, M. Klene, X. Li, J. E. Knox, H. P. Hratchian, J. B. Cross, C. Adamo, J. Jaramillo, R. Gomperts, R. E. Stratmann, O. Yazyev, A. J. Austin, R. Cammi, C. Pomelli, J. W. Ochterski, P. Y. Ayala, K. Morokuma, G. A. Voth, P. Salvador, J. J. Dannenberg, V. G. Zakrzewski, S. Dapprich, A. D. Daniels, M. C. Strain, O. Farkas, D. K. Malick, A. D. Rabuck, K. Raghavachari, J. B. Foresman, J. V. Ortiz, Q. Cui, A. G. Baboul, S. Clifford, J. Cioslowski, B. B. Stefanov, G. Liu, A. Liashenko, P. Piskorz, I. Komaromi, R. L. Martin, D. J. Fox, T. Keith, M. A. Al-Laham, C. Y. Peng, A. Nanayakkara, M. Challacombe, P. M. W. Gill, B. Johnson, W. Chen, M. W. Wong, C. Gonzalez, J. A. Pople, Gaussian, Inc., Pittsburgh, PA, **2003**.
[60] M. Cossi, G. Scalmani, N. Rega, V. Barone, *J. Chem. Phys.* **2002**, *117*, 43–54.

[61] P. Ganesan, J. Baggerman, H. Zhang, E. J. R. Sudholter, H. Zuilhof, *J. Phys. Chem. A* **2007**, *111*, 6151–6156.
[62] J. Baggerman, *Photoactive Hydrogen Bonded Rotaxanes*, Ph. D. Thesis, Universiteit van Amsterdam, **2006**.
[63] B. M. Aveline, S. Matsugo, R. W. Redmond, *J. Am. Chem. Soc.* **1997**, *119*, 11785–11795.
[64] A. Zweig, W. G. Hodgson, W. H. Jura, *J. Am. Chem. Soc.* **1964**, *86*, 4124–4129.
[65] J. Ouyang, A. J. Bard, *J. Phys. Chem.* **1987**, *91*, 4058–4062.
[66] F. A. Carroll, M. T. McCall, G. S. Hammond, *J. Am. Chem. Soc.* **1973**, *95*, 315–318.
[67] I. B. Berlman, *Handbook of Fluorescence Spectra of Aromatic Molecules*, Academic Press, New York, **1971**.
[68] G. Grabner, S. Monti, G. Marconi, B. Mayer, C. Klein, G. Koehler, *J. Phys. Chem.* **1996**, *100*, 20068–20075.
[69] M. Choy de Martinez, O. P. Marquez, J. Marquez, F. Hahn, B. Beden, P. Crouigneau, A. Rakotondrainibe, C. Lamy, *Synth. Met.* **1997**, *88*, 187–196.
[70] P. O'Neill, S. Steenken, D. Schulte-Frohlinde, *J. Phys. Chem.* **1975**, *79*, 2773–2779.
[71] B. Chutny, A. J. Swallow, *Trans. Faraday Soc.* **1970**, *66*, 2847–2854.
[72] J. Holcman, K. Sehested, *J. Chem. Soc. Faraday Trans. 1* **1975**, *71*, 1211–1213.
[73] G. Bottari, F. Dehez, D. A. Leigh, P. J. Nash, E. M. Pérez, J. K. Y. Wong, F. Zerbetto, *Angew. Chem.* **2003**, *115*, 6066–6069; *Angew. Chem. Int. Ed.* **2003**, *42*, 5886–5889.
[74] D. D. Günbaş, A. M. Brouwer, *J. Org. Chem.* **2012**, *77*, 5724–5735.
[75] A. B. C. Deutman, C. Monnereau, J. A. A. W. Elemans, G. Ercolani, R. J. M. Nolte, A. E. Rowan, *Science* **2008**, *322*, 1668–1671.
[76] P. H. Ramos, R. G. E. Coumans, A. B. C. Deutman, J. M. M. Smits, R. de Gelder, J. A. A. W. Elemans, R. J. M. Nolte, A. E. Rowan, *J. Am. Chem. Soc.* **2007**, *129*, 5699–5702.
[77] R. G. E. Coumans, J. A. A. W. Elemans, R. J. M. Nolte, A. E. Rowan, *Proc. Natl. Acad. Sci. USA* **2006**, *103*, 19647–19651.
[78] I. L. Yoon, D. Benitez, Y.-L. Zhao, O. S. Miljanic, S.-Y. Kim, E. Tkatchouk, K. C. F. Leung, S. I. Khan, W. A. Goddard, J. F. Stoddart, *Chem. Eur. J.* **2009**, *15*, 1115–1122.
[79] K. Nikitin, E. Lestini, J. Stolarczyk, H. Müller-Bunz, D. Fitzmaurice, *Chem. Eur. J.* **2008**, *14*, 1117–1128.
[80] D. C. Jagesar, S. M. Fazio, J. Taybi, E. Eiser, F. G. Gatti, D. A. Leigh, A. M. Brouwer, *Adv. Funct. Mater.* **2009**, *19*, 3440–3449.

Received: November 9, 2012
Published online: April 5, 2013

